Bulletin de la Socié Royale des Sciences de Liège - Vol. 74, 1-2-3, 2005, pp. 139-145

Active and adaptive optics for the Carlina Hypertelescope

H. Le Coroller [1], V. Borkowski [1], J. Dejonghe [1]
and A. Labeyrie [1]

[1]LISE-Collège de France, Observatoire de Haute-Provence, France

Abstract: We describe a wave sensing method developed for the diluted aperture of the Carlina hypertelescope (Labeyrie 2002) and other instruments having non-monolithic mirrors. Carlina is configured like a diluted version of the Arecibo radio-telescope. The diluted primary mirror is made of fixed co-spherical segments widely spaced with respect to their size. Above this diluted mirror a helium balloon carries a gondola containing the focal optics and detector. Following the first fringes obtained on Vega with a prototype (Le Coroller et al. 2004), we develop active and adaptive optics expected to respectively coherence and phase several tens of mirrors.

1 Introduction

Interferometers such as VLTI, IOTA, CHARA, etc... commonly use more than just two sub-apertures. For example, IOTA observes with three telescopes while CHARA will soon work with six telescopes. Their baselines reach a few hundred meters. The next-generation interferometers will increase the baseline up to 1-10 km. The number of apertures also needs to be increased as much as possible: to obtain an image with N^2 resels, N non redundant mirrors are needed.

The cost and complexity of the conventional interferometers are significantly increased by the delay lines (Mourard et al. 2003). The architecture of Carlina is more simple in its conception (Le Coroller et al. 2002). Carlina is analogous to the Arecibo radio telescope, although it uses a diluted spherical primary mirror which consists in many small mirrors, widely spaced with respect to their size. They have a shallow spherical curvature and are carried co-spherically by fixed supports inside a naturally concave site, canyon or crater. Above the diluted primary mirror, a helium balloon carries a gondola equipped with the focal optics and detector (see Fig. 3). The absence of delay lines is a major simplification, paving the way towards using hundreds or thousands of mirrors for producing images with rich information content. This type of hypertelescope has been previously described by Labeyrie et al. (2002).

Recently, we obtained the first fringes on Vega with a Carlina prototype built at the Haute-Provence Observatory (Le Coroller et al. 2004). The initial testing configuration used only two close mirrors on the ground and the fringes were obtained in Fizeau mode. In section 2, we describe how we co-spherized the two mirrors of this prototype. In section 3, we discuss a co-sphericity sensor at the curvature center for Carlina's active optics. In section 4, we focus on the adaptive optics in the gondola using the "dispersed speckles" method to cophase the mirrors.

2 Coherencing the Carlina prototype

A hypertelescope is a multi-element interferometer equipped with a pupil densifier to do direct imagery. The densified pupil allows to concentrate much of the light, usually dispersed in secondary peaks, in the central one. It consists in increasing the ratio of sub-aperture diameters to their spacing, in order to make the sub-pupils almost contiguous, while preserving the pattern of their centers. The advantage of a hypertelescope mode, rather than Fizeau, imaging mode on multi-aperture interferometers is the higher luminosity of the direct high resolution images.

The pupil densification shrinks the size of the envelope containing the interference pattern. It also shrinks the celestial field of view to λ/s (where s is the sub-aperture spacing). A diluted mosaic of such "Direct Imaging Fields", spaced by λ/d on the sky (where d is the sub-aperture size) is however obtainable by using an array of tiny pupil densifiers, similarly spaced. For example, if we consider a collecting area of 7,000 m^2, diluted across a 1.5 km "sparse aperture", its resolution is improved 15 times, but the Direct Imaging Field (also called Zero Order Field if the aperture is a periodic grating-like array) is shrunk to 0.007 arc-second in yellow light if the sub-apertures are 1 meter in size and spaced by 15 meters. With an array of densifiers, possibly built with integrated optics techniques, the multiple fields are spaced by 0.1 arc-second, the size of the sub-aperture lobes. Within each field, the image contains 836 X 836= 7,000 resels. The total number of sky sources within the larger sub-aperture lobes should not exceed this resel number to avoid a crowding effect affecting the image contrast. However, if the aperture is redundant, the image remains usable with a source count per lobe reaching the square of the aperture count, i.e. 49 million in the example considered. The number of fields, limited by the off-axis aberrations of the diluted telescope, can exceed several millions, especially if static aberration corrections are incorporated in the pupil-densifiers located off-axis. A continuous mosaic image is obtainable from a sequence of exposures made at incremental pointing coordinates. The drawback is a limitation of the Direct Imaging Field of view, but the multi-densifier techniques recover much of the field, and all of it with multiple exposures.

The co-spherizing method used for adjusting the Carlina prototype built at the Haute-Provence Observatory was described in much detail by Le Coroller et al. (2004). Here, we only give some more details and illustration of this method.

The two close primary mirrors where adjusted in co-sphericity, within a micron, with an optical system placed at the curvature center. A flat folding mirror covering parts of both mirror segments makes the curvature center easily accessible at ground level (see Fig. 1). A point source is placed at this "folded" curvature center, near a CCD camera receiving the two returning images of the light source produced by the primary segments. Using the three micrometric screws which carry each mirror element, we then adjust the tip-tilt by superimposing these two images. The piston is adjusted by searching the Young's fringes and centering them in the image, as well as the turbulence-induced jitter allows.

When we find the fringes, the piston error between the mirrors is comparable to the coherence length of the source, which can be a diode laser initially for coarse adjustment. The laser source is then replaced by a white source to increase the piston sensitivity down to the seeing-limited value, decreasing below one micron when averaging visually for a few minutes. With this method, we adjust the primary mirrors on the virtual giant spherical surface without stellar light. Then we can directly point the star by moving the gondola along the focal sphere (Coroller et al., 2004), and the fringes appear immediately, as shown on Fig. 2. Although the tracking jitter, resulting from wind, the elasticity of the cables, and the computer-controlled winches, moves the balloon-suspended focal camera by one or several millimeters relative to the image, this does not move the fringes with respect to the image envelope. Only "seeing" does, since the bed-rock supporting the primary mirrors ensures excellent short-term stability. Unlike previous interferometers, this makes servo-loops unnecessary for the initial observations in the speckle interferometry mode if a fast camera is used. It will also simplify

Figure 1: *Initial testing configuration with two 25cm mirrors arranged in close spacing and a folding flat mirror for metrology at the curvature center. The two spherical mirrors are partially covered by the flat mirror making the curvature center easily accessible at ground level, 70 meters away. The mirror supports are rigidly anchored to the bed-rock via concrete and carbon fiber tubes.*

the adaptive optics, particularly for piston adjustments.

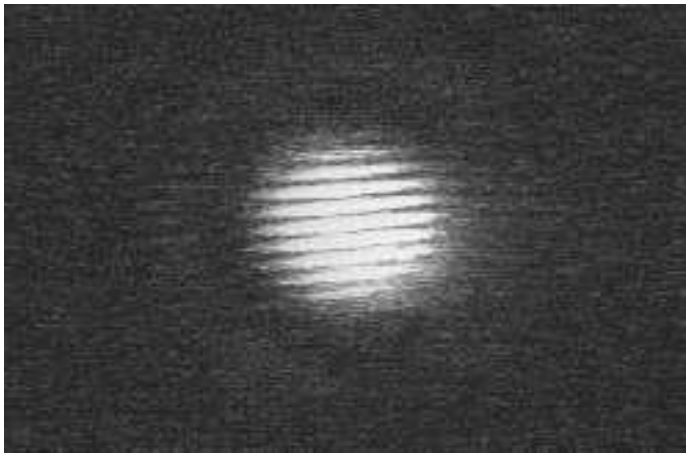

Figure 2: *First fringes with Carlina prototype, obtained on Vega in May 2004.*

With the flat mirror covering only a small part of both spherical mirrors, it is possible to observe the star and to monitor the metrology fringes at the curvature center simultaneously. Moreover, the bedrock stability is sufficient to keep the primary segments in coherence, within microns, for days, depending on weather conditions, mainly temperature and humidity. The folding flat mirror obviously cannot be large enough to work with primary mirrors located far apart, in which case the metrology source and camera must be suspended at the curvature center of the large diluted mirror (see Fig. 3).

A large ring of close mirrors can however conceivably be co-spherized with reasonably small flat mirrors covering each pair of adjacent segments, the piston and tip-tilt of mirror $N+1$ being adjusted with respect to mirror N. But this technique adds the phasing errors. Once the primary mirror elements are co-spherized, the clam-shell corrector of spherical aberration must be aligned. It is internally pre-aligned in the laboratory, together with the pupil densifier and camera attachments. But its three translations and two rotations, with respect to the primary optics and star direction, must be aligned within the gondola. The tolerances are of the order of millimeters in translation and arc-minutes

in tip-tilt. They can be met by simple methods, to be explained in another article. In comparison with the metrology techniques utilized for existing interferometers, this internal metrology method for Carlina architectures is appreciably simplified. Unlike the direct piston sensing also achievable on the stellar wavefront (Sect. 4), this metrology technique ignores the possible additional piston errors introduced by the atmosphere. The corrector being separately tested however, and its alignment errors monitored, the curvature-center metrology can allow blind coherencing for observations of rather faint stars in the speckle interferometry mode. Accurate metrology of course reduces the dispersion needed in the "dispersed speckle" analyzer discussed below, which makes it more sensitive for phasing faint objects.

3 Active optics for Carlina

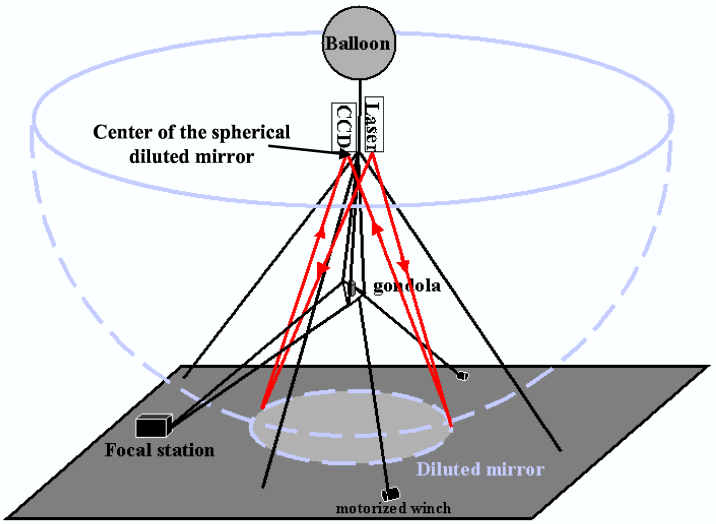

Figure 3: *Carlina is configured like a diluted version of the Arecibo radio telescope. The primary mirror is made of fixed co-spherical segments. The gondola moves on the half-radius focal sphere to track the stars, using a cable suspension which ensures equatorial tracking with a single computer-controlled winch (Le Coroller et al. 2004). A co-spherisation sensor is placed at the curvature center of the primary mirror.*

Using the procedure described in the previous section the mirrors can be co-spherized pairwise. But co-spherizing simultaneously several mirrors, and possibly many, requires a wavefront sensor capable of dealing with diluted apertures, which is not the case for the conventional sensors of slope or curvature errors. The "dispersed speckles" method (see Sect. 4) can be applied, either in a star image at the focal plane in the gondola or in the image of a white point source at the curvature center. The latter version monitors only the co-sphericity of the primary elements, not the focal corrector nor the turbulence affecting the stellar wavefront. It involves an optical system that creates an (x, y, λ^{-1}) cube, obtained with a spectro-imager giving a series of speckled images of the white source at different wavelengths. The algorithm then calculates the piston errors from this input data cube.

If utilized at the curvature center, the white source can be replaced by a laser source emitting staged wavelengths cyclically, to build the input cube without a spectro imager. The piston measurement acuracy improves in proportion to the spectral width. For example: with an optical bandwidth of 400 nm, a wavelength of 550 nm, a 8 non redundant apertures interferometer and 960 photons, the precision reaches 0.2 μm (Borkowski et al. 2004). However, this optical device at the curvature center cannot be used for the adaptive optics since the star light does not follow the same path through

the atmosphere as the light coming from the curvature center. For the adaptive optics the wavefront sensor described in Sect. 4 must be placed in the gondola at the Fizeau or densified focus of the interferometer and uses the star light.

4 The dispersed speckle method for cophasing

The wave sensors using slope or curvature measurements are suitable for monolithic telescopes or segmented ones but not for diluted interferometers.

The "dispersed speckles" method, proposed by Labeyrie (2002) and described in further detail by Borkowski et al. (2004), Martinache (2004), Borkowski (2004), is a multi-aperture generalization of the time-honored dispersion method used since Michelson, at least, to find and center two-aperture fringes. The "mange-frange" method developed for the GI2T at Calern (France) by L. Koechlin (Koechlin et al. 1996) is a computerized version of the traditional method, which analyzes the dispersed fringes on-line, using a 2-dimensional Fourier transform to extract the fringe slope signal. The "dispersed speckle" method can exploit many apertures by using a 3-dimensional Fourier transform to calculate the piston errors among the sub-apertures. We briefly recall its principle and properties.

4.1 The principle

The first step is to record a series of monochromatic images at different wavelengths at the focus of a N apertures interferometer, here assumed non-redundant, and pile-up these images so as to build a cube, the third dimension of which is the wavenumber. The second step consists in calculating a 3-dimensional Fourier transform of this "input cube", once corrected for the speckle's size chromatism. The resultant cube called "output cube" contains $N(N-1)$ signal dots, arrayed centro-symetrically and which move along vertical columns in response to piston variations. The output cube dots are located in "active columns". Scanning one active column to find the signal dot gives the piston value for one pair of sub-apertures. Only $N(N-1)/2$ signal dots are needed to retrieve all the pistons. The projection of these dots positions on the median horizontal plane of the cube matches the autocorrelation points of the entrance pupil. If the aperture is redundant, each column can contain several dots. Solving for piston errors in such conditions remains possible with the methods discussed by Martinache (2004).
As an example, simulations have shown that with 8 non-redundant apertures, 960 photons are needed to measure piston values.

After these encouraging results, we built a prototype instrument to validate the dispersed speckles method (Borkowski V. and Labeyrie A. 2004).

4.2 The dispersed speckles piston sensor

The optical setup of the dispersed speckles piston sensor is sketched in Fig. 4. As can be seen in the middle part of this figure, the aperture formed by multiple holes, is placed just before the first lens L_1. An image of an artificial star is formed in the image plane S'. A pupil P' is just after the microscope objective L_2. A strongly magnified image S" is located on L_3. The magnification, $\times 50$ in this case, is such that the speckle size matches the size of the multi-faceted deviating wedge's facets, 5×5 mm. The multi-faceted deviating wedge (elsewhere called multi-prism) has two crossed arrays of 10×10 slides tilted with incremental angles. It generates 100 prismatic facets having different angles but parallel ridges. These explode the spectrum into parallel spectra, one for each speckle,

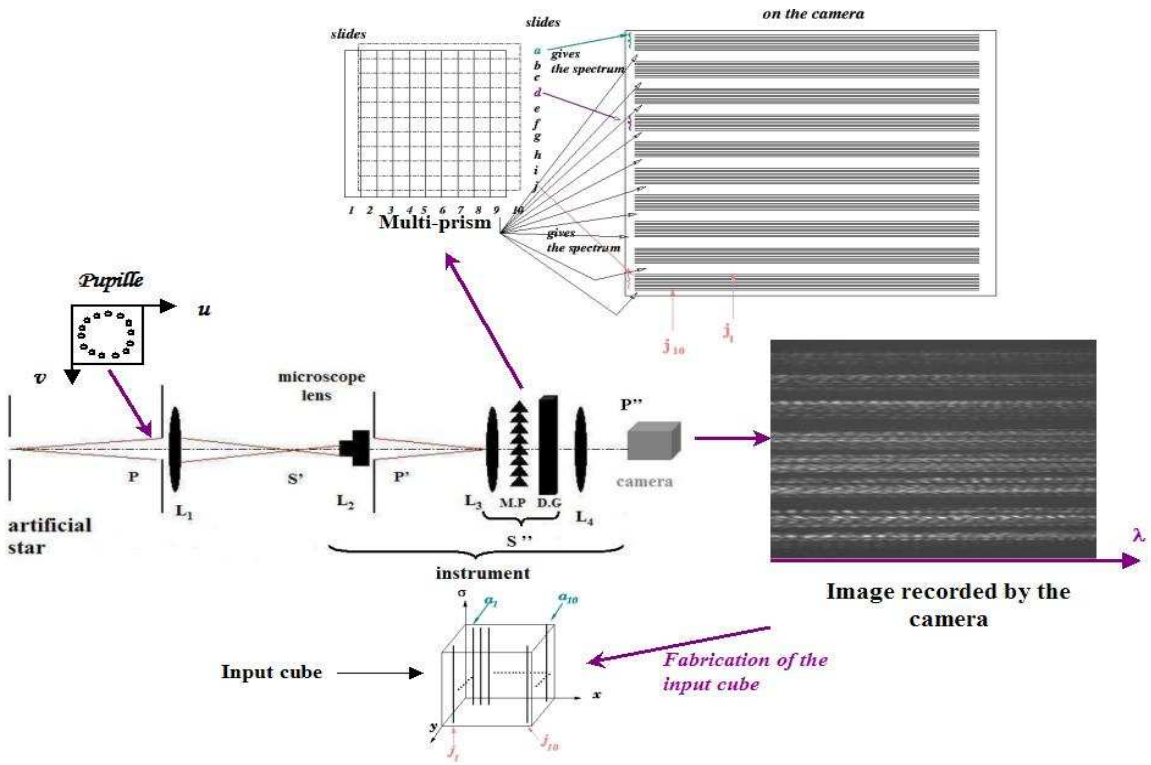

Figure 4: *Prototype of the dispersed piston sensor built in laboratory.*
On top and from left to right: multi-faceted deviating wedge having 10 × 10 facets and the series of spectra recorded by the camera. On the middle: optical setup and image recorded by the camera. At the bottom: input cube built from the recorded image.

suitably arrayed on the CCD camera (see top right part of Fig. 4). The transmissive diffraction grating disperses the light of each speckle, projected on the grating at strong magnification, the tiny pupil upstream serving as the slit of the spectrographic setup. The lens L_4 focuses the pupil on the camera. The first spectrum in the upper part of the CCD is produced by a speckle located on the M.P facet a_1. This setup allows to build the input cube needed for the dispersed speckles method.

Other types of spectro-imaging optics, such as the Courts field-grating scheme and those using a grating near a micro-lens array in the image plane, are also potentially usable.

5 Conclusions

In this article, we outline design solutions for the active and adaptive optics of Carlina hypertelescopes. We have shown that the mirrors of Carlina can be co-spherized with sub-micron accuracy without stellar light, using the "dispersed speckle" method with a metrology source and sensor located at the curvature center. The focal corrector of spherical aberration being pre-adjusted, in the laboratory or when observing a bright star, this allows blind coherencing on faint stars for speckle interferometric observing. The stability of the primary mirror's co-spherization is limited by the bed-rock drift, typically well below that of component telescopes in multi-telescope interferometers. Imperfect tracking by the focal optics causes mostly image jitter on the camera, without degrading the image if short exposures are used. We also describe the adaptive optics achievable by sensing piston errors on the star, using again the "dispersed speckles" method. With these methods, the Carlina architecture is expected to become usable with effective aperture sizes from 1 to 2 km. In space, much larger sizes of

1 km, 100 km and 100,000 km appear achievable (Labeyrie, 2004; Labeyrie: Formation Flying conf. Washington DC, 2004, http://durance.oamp.fr/lise/biblio.html).

Acknowledgements

We would like to thank the staff at the Observatory of Haute-Provence for its help.

References

Borkowski V. 2004, thesis, University of Nice-Sophia Antipolis.
Borkowski V., Labeyrie A., Martinache F. and Peterson D., A&A 2004 (in press).
Borkowski V. and Labeyrie A. 2004, ESA Publication Series, C. Aime ed., in press.
Koechlin L. et al. 1996, Applied Optics, 35, pp.3002-3009.
Labeyrie 2004, proc. SPIE Glagow.
Labeyrie A. et al. 2002, Proceedings of the SPIE, Vol. 4852, pp. 236-247.
Labeyrie A. et al 1996 A&A Suppl. Series, v.118, pp.517-524.
Lardière O. et al. 2002, ASP Conference Series, vol. 266. Edited by J. Vernin et al., Astronomical Society of the Pacific, p.608
Le Coroller A. et al., A&A 2004, 426, 721-728.
Mourard D. et al. 2003, Interferometry for Optical Astronomy II, ed. A. Wesley Traub, Proc. SPIE 4838, 9.